Mapping Electric Organ Discharges of Weakly Electric Fish

*Maximilian Seligman, *Jennifer Hunt, Louis Bran, Carmen-Jeanette Stepek, Celina Valladarez, Triston Millstone, Jonathan Granados, Dr. Brian Rasnow

*These authors made equal contributions

Introduction

Weakly electric fish have an electric organ that generates an electric field called its electric organ discharge (EOD). The EOD is used for intraspecific communication, prey detection, and localization in its environment.

We have created an apparatus to robotically map and study EODs in a fish tank. With it, we hope to better understand this foreign sense of animal perception and the biophysics underlying it. Electric fish are model biological systems, much simpler to study and manipulate than mammals and humans. We expect that insights into electroreception will likely reveal general evolutionary principles of neuroethology that apply to other animals including us [Rasnow 2014].

Methods

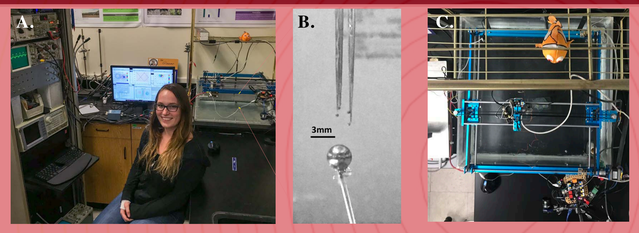

Figure 1. Apparatus consists of a 3D Cartesian robot (right A and C, top view) that moves a small array of fine silver electrodes (B) around a fish tank. Analog amplifiers (left C) send voltages to a high fidelity data acquisition system in a PC (bottom left A). Other equipment in the rack include an oscilloscope, amplifiers, and multiple signal sources (left A).

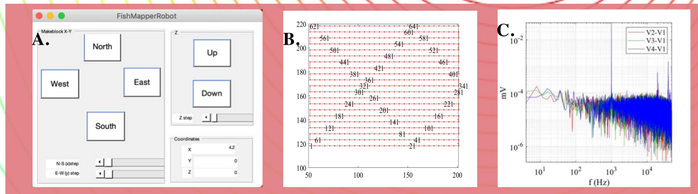

Figure 2. The apparatus is controlled through MATLAB. The robot is driven by 2 Arduinos communicating through serial strings generated by scripts and a simple Graphic User Interface (GUI) (A). Numerous scripts and functions generate mapping sequences (B), execute the maps, and analyze as well as visualize the data. Voltages are digitized simultaneously on 5 channels at 100,000 24-bit samples per second. Fourier transforms reduce this voluminous data at each location and channel to a single complex number representing the waveform's amplitude and phase. Amplitude spectrum of the voltage differences between the 4 array electrodes are shown in (C).

Calibration: The apparatus was calibrated by mapping dipole potentials as well as fields and comparing them to theory (Figs. 3-4). Electromagnetic theory predicts that a physical dipole with poles located at $\vec{p}_1, \vec{p}_2$, in an infinite fish tank will produce an electric field and electric potential given by:

$$\vec{E}(\vec{x}) = \frac{\rho I}{4\pi}\left(\frac{\vec{x}-\vec{p}_1}{|\vec{x}-\vec{p}_1|^3} - \frac{\vec{x}-\vec{p}_2}{|\vec{x}-\vec{p}_2|^3}\right) \quad \text{(Eqn. 1)} \qquad V(\vec{x}) = \frac{\rho I}{4\pi}\left(\frac{1}{|\vec{x}-\vec{p}_1|} - \frac{1}{|\vec{x}-\vec{p}_2|}\right) \quad \text{(Eqn. 2)}$$

ρ is the water resistivity and *I* is the current. A pair of electrodes located at $\mathbf{x}_1$ and $\mathbf{x}_2$ will measure a potential difference, $V_2 - V_1 = -\vec{E}\cdot(\vec{x}_2 - \vec{x}_1)$. Potential differences between 3 non-planar electrodes at $\vec{x}_k = (x_k, y_k, z_k)$ are related to the local electric field vector by the interelectrode distance matrix:

$$\begin{bmatrix} V_2-V_1 \\ V_3-V_1 \\ V_4-V_1 \end{bmatrix} = -\begin{bmatrix} x_2-x_1 & y_2-y_1 & z_2-z_1 \\ x_3-x_1 & y_3-y_1 & z_3-z_1 \\ x_4-x_1 & y_4-y_1 & z_4-z_1 \end{bmatrix}\begin{bmatrix} E_x \\ E_y \\ E_z \end{bmatrix} \quad \text{(Eqn. 3)}$$

Inverting Eqn. 3 determines the electric field components from the measured potential differences (Fig. 5B).

Two optimizations were performed to calibrate unknown parameters. First, the pole locations at $\vec{p}_1, \vec{p}_2$, were nudged to minimize the squared error between measurements and Eqn. 2. Secondly, the interelectrode matrix (Eqn. 3, actually its inverse) was found by minimizing the error between 651• 3 differential voltage measurements and Eqn. 1.

Validation: Using these previously determined parameters, we repeated potential and field maps, computing means and standard deviations. Additionally, we computed a field component by subtracting potentials measured at adjacent positions and compared these with differential recordings (Fig. 6).

Results

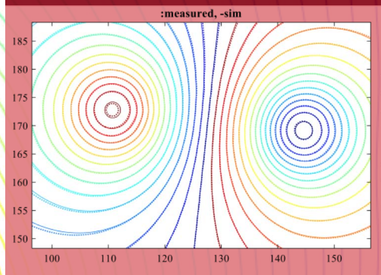

Figure 3. Dotted contours are 100 μV equipotentials interpolated from measurements at 651 locations ~10mm above the dipole (x and y axes are robot coordinates in mm). Solid contours are 100μV equipotentials of a simulation with Eqn. 2. The only free parameters were small adjustments made to the locations of the two poles, found with a simplex optimization:

```
err = @(poles) sum((monopole(fp, poles,...
   strengths)-pot1).^2); % squared error
bestPoles = fminsearch(err, initPoles, opts);
```

where `monopole` implements Eqn. 2 and `fp` are the coordinates corresponding to data `pot1`.

Figure 4. Visualization of 3D electric field vectors is challenging. Here, we represent field vectors at 651 planar locations as arrows with components (Ex, Ey), superimposed on contours of equal Ez. Red arrows and dotted contours are from array measurements; theory are blue arrows and solid contours. At this phase, the field diverges from the left pole, pointing towards you. Halfway between the poles, Ez is zero as the field vectors turn from outward to inward, toward the right pole. Colorbar shows Ez units (mV/mm). Close agreement between theory and experiment was achieved by optimizing the interelectrode distance matrix as described in the next figure.

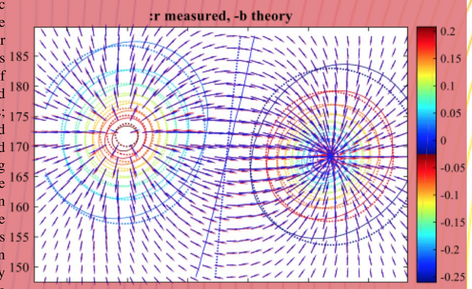

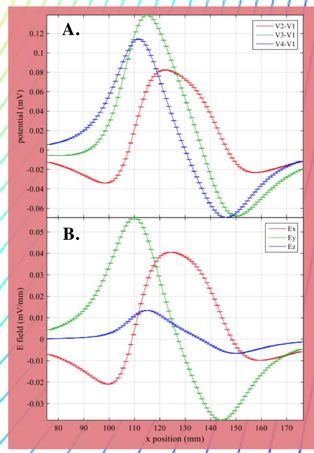

Figure 5. Interelectrode potential differences were measured at 100 points 1mm apart, parallel to the dipole (in < 1.5 minutes) and these measurements were repeated 4 times. Means and standard deviations are shown (A). The Cartesian electric field components along this path (B) were computed by multiplying this data by the inverse of the interelectrode distance matrix (in mm):

```
>> inv(bestparams(1:3,:))
ans =
    1.8947    0.1472    0.3840
    2.0848    2.2393   -1.7217    (Eqn. 4)
    0.3236    1.7632    1.0073
```

found by a second simplex optimization:

```
monopoleErr = @(p) sum((sum((v2e(dv,p,5) - ...
  monopoleE(fp, bestPoles, strengths)).^2,2)));
bestv2emat = fminsearch(monopoleErr, p, opts);
```

where `v2e` implements Eqn. 3 and `monopoleE` implements Eqn. 1.

Repeating the map of Fig. 4 multiple times resulted in an average interelectrode spacing (Eqn. 4) ~1.2mm and a repeatability ~20 microns or a few percent.

Figure 6. The x-component of the electric field was measured with two techniques. The red curve is the result of differential measurements from the array processed through the optimized interelectrode distance matrix. The green curve represents the differences in potential of a single electrode measured at adjacent positions divided by the 1mm robot steps,

i.e., $\frac{-(V(\vec{x}_2)-V(\vec{x}_1))}{|\vec{x}_2-\vec{x}_1|}$

Greater noise in the green curve is likely due to robot jitter, which does not affect interelectode distances of the rigid array.

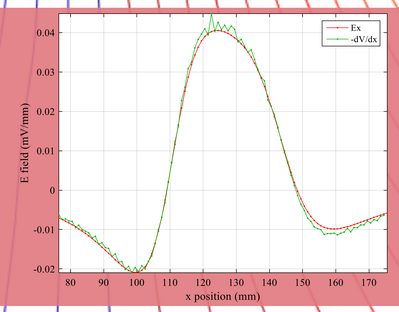

Background: interpolated 30uV isopotentials measured above the dipole.

Discussion

We have demonstrated the capability to map weak electric potentials and field vectors in a fish tank with remarkable accuracy, precision, and speed. Voltage amplitude noise is ~100nV (Fig. 1C), thus a typical EOD of ~10mV may be measured with a precision of 10^{-4}. This is approximately an order of magnitude better than prior measurements, and within an order of magnitude of a fish's sensitivity thresholds (determined by behavioral experiments). The array measures field vectors with comparable precision (Fig. 5) at a rate moderately faster than one position per second. Amplitude accuracy is generally around 1% (Figs. 4 and 6). The dipole field calibrated our apparatus and provided confirmation that our maps are accurate. When we map a fish's EOD, the sources are more complex (and unknown), but we can now be confident that the fields we measure are real.

These measurements were done with a voltage across the dipole ~14mV rms and current ~6.7μA rms, power ~0.1 microwatts distributed in the tank. This is comparable to what these fish sense.

Throughout this project, we overcame many challenges. Getting noise levels this low required identifying and eliminating numerous noise sources, including ground loops, USB interference, and most significantly, disabling the robot's stepper motors when they are not moving. Repurposing this robot (designed as a printer) as an EOD mapper involved numerous dives into its complex hardware and software.

Noise was also reduced by Fourier filtering the data to a bandwidth of a few Hz. Some fish's EODs are the most stable biological oscillators, so this method can be applied separately to their fundamental and lower harmonic frequencies. "Pulse-type" electric fish do not have discrete harmonics, so other signal processing methods will be used, e.g., based on cross-correlations in the time domain.

Adaptability and ease of use are key features of an apparatus to study animals. A prerequisite for mapping fish is to achieve enough practice, skill, and understanding of the apparatus and its interfaces, so mistakes that invalidate the experiment are not made. Most of the data presented here was collected during a single session lasting a few hours. The acquisition time for both Figs. 3 and 4 was <15 minutes, Figs. 5 and 6 took <1.5 minutes for each repetition. The precondition for this productive experiment were numerous prior attempts at mapping and analysis that built our skills and understanding, along with continuing refinements to the apparatus. We have written dozens of concise MATLAB scripts and functions simplifying common tasks. We have modified hardware and Arduino firmware so the robot moves fast and generates no electrical interference when it is stationary. Future additions include incorporating video monitoring of the fish and completing a respiration system to keep it alive while paralyzed or sedated.

Future experiments have the expectation to reveal, for the first time, the electric environments of several species of fish previously unstudied at this level of resolution. We also plan to explore biophysical characteristics of the EOD, such as how much power is actually in the fish's field, as the current literature contains ambiguities [Salazar et al. 2013].

Summary

- Weakly electric fish generate an *extremely* weak electric field that is imperceptible to humans
- We have constructed an apparatus that rapidly and accurately maps this field
- We have developed robust methods to calibrate the apparatus using a dipole signal source
- Our control, analysis, and visualization software is versatile and flexible
- We gained valuable experience with systematic troubleshooting
- We learned about experimental design and posing beneficial and important questions
- We developed skills to bridge various practical disciplines of science in a laboratory setting

Literature Cited

Rasnow B (2014) Electricity, eels and evolution. Review of Turkel, W. Spark from the Deep. Physics World 27(7):44-5.

Salazar VL, Krahe R, Lewis JE (2013) The energetics of electric organ discharge generation in gymnotiform weakly electric fish. J. Expt. Biol 256:2459-2468.

Acknowledgements

We would like to thank Dr. Ruben Alarcón for granting us access and allowing us to use his lab space.

We thank Brian J. Clark for the donation of the robot (plotter).